Received: 14 December 2022 | Revised: 24 January 2023 | Accepted: 21 February 2023

DOI: 10.1002/biot.202200622

Biotechnology Journal

RESEARCH ARTICLE

Catalytically self-sufficient CYP116B5: Domain switch for improved peroxygenase activity

Danilo Correddu[1] | **Gianluca Catucci**[1] | **Daniele Giuriato**[1] | **Giovanna Di Nardo**[1] | **Alberto Ciaramella**[1,2] | **Gianfranco Gilardi**[1]

[1]Department of Life Sciences and Systems Biology, University of Torino, Torino, Italy

[2]HuvePharma Italia, Garessio, Italy

Correspondence
Gianfranco Gilardi, Department of Life Sciences and Systems Biology, University of Torino, Via Accademia Albertina 13, 10123 Torino, Italy.
Email: gianfranco.gilardi@unito.it

Abstract

Self-sufficient cytochromes P450 of the sub-family CYP116B have gained great attention in biotechnology due to their ability to catalyze challenging reactions toward a wide range of organic compounds. However, these P450s are often unstable in solution and their activity is limited to a short reaction time. Previously it has been shown that the isolated heme domain of CYP116B5 can work as a peroxygenase with H_2O_2 without the addition of NAD(P)H. In this work, protein engineering was used to generate a chimeric enzyme (CYP116B5-SOX), in which the native reductase domain is replaced by a monomeric sarcosine oxidase (MSOX) capable of producing H_2O_2. The full-length enzyme (CYP116B5-fl) is characterized for the first time, allowing a detailed comparison to the heme domain (CYP116B5-hd) and CYP116B5-SOX. The catalytic activity of the three forms of the enzyme was studied using *p*-nitrophenol as substrate, and adding NADPH (CYP116B5-fl), H_2O_2 (CYP116B5-hd), and sarcosine (CYP116B5-SOX) as source of electrons. CYP116B5-SOX performs better than CYP116B5-fl and CYP116B5-hd showing 10- and 3-folds higher activity, in terms of *p*-nitrocatechol produced per mg of enzyme per minute. CYP116B5-SOX represents an optimal model to exploit CYP116B5 and the same protein engineering approach could be used for P450s of the same class.

KEYWORDS
CYP116, cytochromes P450, domain switch, H_2O_2, peroxide shunt, peroxygenase

1 | INTRODUCTION

Cytochromes P450 are heme containing enzymes of high interest in biotechnology as they catalyze a variety of oxidation reactions of an extraordinary number of different types of molecules.[1,2] They are present in nearly all organisms and are classified based on the structural arrangement of their functional domains.[3] Typically, the heme containing domain carries out its catalytic activity in coordination with a separate reductase domain, which accepts electrons from an external donor and transfers them to the heme for the catalytic cycle.[4,5] However, the use of such systems for biotechnological purposes is not cost effective due to the price of the reduced electron donors and can be limited by the poor solubility and stability of the proteins. To overcome these problems, recent developments on enzyme biotechnology point toward the use of the so-called self-sufficient cytochromes P450 that carry out their function independently.[6,7] There are two types of

self-sufficient P450s, class VII and class VIII, in which the heme containing domain and the reductase domain are fused in the same polypeptide chain, and class IX and X consisting of a heme containing domain that can accept electrons directly from a donor such as NAD(P)H and H_2O_2 or via an intramolecular arrangement.

Among class VIII, the most studied self-sufficient cytochrome is CYP102A1 (P450 BM3), a highly efficient fatty acid hydroxylase from *Bacillus megaterium*.[8] Indeed, the great catalytic performance of P450 BM3 and the use of the same type of enzymes for industrial applications is limited by the narrow substrate scope and by the need for the expensive cofactor NAD(P)H. Nevertheless, P450 BM3 has been successfully engineered to expand the range of its reactivity toward other types of molecules such as pharmaceuticals and aromatic compounds.[9–14] Most interestingly, a different approach was used to develop new mutants of P450 BM3 in which an efficient catalysis could be driven by H_2O_2 via the so-called peroxide shunt.[15–17] This pathway is typical of a special group of P450 peroxygenases[18] such as CYP152B1 (SPα)[19] and CYP152L1 (OleTJE).[20] However, enzymes that carry out their catalysis via the peroxide shunt have a limited lifetime due to the destabilization and the damage caused by H_2O_2. As for class VII, these cytochromes P450 are emerging as powerful biocatalysts thanks to their wide substrate scope, ranging from simple molecules such as fatty acids, to more complex molecules such as polycyclic hydrocarbons, pesticides, and drugs.[6] Cytochromes of this class are well represented by bacterial enzymes of the sub-family CYP116B, which are mostly present in extremophile microorganisms that can live under extreme temperature or radiations, high salinity, or in the presence of toxic molecules.[21–28] Class VII cytochromes are well represented by CYP116B5 from *Acinetobacter radioresistens*. This P450 was first identified and studied in our laboratories.[29] Subsequently, its heme domain (CYP116B5-hd) was expressed, purified, and characterized, revealing a high tolerance to H_2O_2 and an extraordinary ability to work as a peroxygenase by using the peroxide shunt,[30,31] despite maintaining the characteristics of a monooxygenase.[32,33] The recombinant production of the heme domain represented an advantage also in terms of solubility, stability, and production yield. On the other hand, although the ability to carry out the catalysis via the peroxide shunt using H_2O_2 instead of NAD(P)H represents a great advantage in terms of costs, the comparison of the catalytic parameters with its full-length form was still missing.

In this work, we expressed and characterized for the first time the full-length form of CYP116B5 from *A. radioresistens*. The properties of the full-length enzyme are used as a term of comparison for protein engineering studies in which the heme domain of CYP116B5 and a monomeric sarcosine oxidase (MSOX) that is able to produce H_2O_2 with a controlled and continuous release in time. The resulting chimeric enzyme (CYP116B5-SOX) exploits the peroxygenase activity of the heme domain sustained by the MSOX domain. The most important outcome is the switching of the P450 reductase partner, which is replaced by MSOX from *Bacillus* sp. B0618, capable of producing H_2O_2, formaldehyde, and glycine starting from sarcosine.[34,35] A comparison of the catalytic properties of the three versions of the enzyme (native full length of CYP116B5, its isolated heme domain and the CYP116B5-SOX chimera) was carried out to establish optimal conditions for biocatalysis.

2 | MATERIALS AND METHODS

2.1 | Bacterial strains, culture conditions, and expression vectors

Escherichia coli supercompetent cells were purchased from Thermo Fisher Scientific (Waltham, MA, USA). *E. coli* DH5α supercompetent cells were used for cloning and plasmid replication. *E. coli* BL21 (DE3) supercompetent cells were used for protein expression trials and large-scale expression. Cells were routinely grown in Luria-Bertani (LB) medium supplemented with 50 μg mL^{-1} of kanamycin at 37°C unless stated otherwise. The DNA sequence of CYP116B5 in its full-length form (GenBank No. HQ685898.1) was cloned into the expression vector pET30a (+). The sequence coding for a poly-histidine tag was also added at the 5′ of the gene for affinity purification purpose. The expression vector containing the coding sequence of CYP116B5 heme domain (CYP116B5-hd) was designed and constructed previously.[31] The DNA sequence of the MSOX from *Bacillus* sp. B0618[36] was cloned into the expression vector pET30a (+), inserting a GPGGGGGGGPG loop between the two functional units, which was previously designed in our lab,[37] and a poly-histidine tag at its C-terminus. Plasmid construction for the expression of the chimeric enzyme CYP116B5-SOX was performed by GenScript (Piscataway, NJ, USA).

2.2 | Protein expression

Expression of CYP116B5-hd was performed as previously published.[31] The expression of CYP116B5-fl was tested using *E. coli* BL21 (DE3) in LB medium supplemented with kanamycin. Overnight cultures were diluted to an OD_{600nm} of about 0.05 in 10 mL cultures. When the OD_{600nm} reached 0.4 the medium was supplemented with 0.5 mM δ-aminolevulinic acid (δ Ala) and 0.05 mM riboflavin. When the OD_{600nm} reached 0.6, the expression of the gene was induced by adding different concentrations of isopropyl β-D-thiogalactoside (IPTG) (0, 0.1, and 1 mM) at different temperatures (28 and 16°C). The cells were grown overnight, harvested by centrifugation for 30 min at 4°C, and resuspended in buffer containing 50 mM potassium phosphate (pH 6.8), 100 mM KCl, 10 mM imidazole, and protease inhibitor cocktail (Roche, Basel, Switzerland). The cells were lysed by sonication and the lysate was cleared by centrifugation for 30 min at 4°C. Whole cell samples and cell-free extracts were analyzed and compared by SDS-PAGE. In order to ensure the same concentration of proteins were being analyzed, whole cell samples were diluted with H_2O according to their optical density.

Expression of CYP116B5-SOX was carried out using *E. coli* BL21 (DE3) in media supplemented with 25 μg mL^{-1} of kanamycin. A single colony was used to inoculate 10 mL of LB medium supplemented with 25 μg mL^{-1} of kanamycin and incubated at 37°C with 220 rpm shaking for 18 h. Five milliliters of the overnight culture were used to inoculate 400 mL TB medium supplemented with 25 μg mL^{-1} of kanamycin. 0.5 mM δ Ala and 50 μg mL^{-1} riboflavin were added as heme and FAD precursors, respectively. Cultures were incubated at 37°C with 180 rpm shaking. When the OD_{600nm} reached 0.4–0.5, the expression of CYP116B5-SOX was induced by adding 0.125 mM IPTG, and the cultures were incubated at 25°C for 24 h. Cells were harvested by centrifugation at 4200 rpm for 30 min.

2.3 | Protein purification

Five hundred milliliters of LB medium supplemented with kanamycin were inoculated with 5 mL of overnight cultures and incubated at 37°C with 180 rpm shaking. When the OD_{600nm} reached 0.4 the medium was supplemented with 0.5 mM δAla and 0.05 mM riboflavin. When the OD_{600nm} reached 0.6, the cultures were grown overnight at 16°C with 180 rpm shaking (without IPTG). Cells were harvested by centrifugation at 4500 rpm for 1 h at 4°C. Cell pellets were resuspended in a lysis buffer containing 50 mM potassium phosphate (pH 6.8), 100 mM KCl, 10 mM imidazole, 5% v/v glycerol supplemented with protease inhibitor cocktail (Roche, Basel, Switzerland) and DNase I, with a 1:5 ratio (g of pellet:mL of buffer). Cells were lysed by sonication and the lysate was clarified by centrifugation at 40,000 rpm for 1 h at 4°C. Poly-histidine-tagged P450 was purified by affinity chromatography using His-Trap HP column (GE Healthcare, Chicago, IL, USA). The column was equilibrated with 10 mL of lysis buffer and washed with the same buffer containing 50 mM imidazole. Poly-histidine-tagged P450 was eluted with a buffer containing 500 mM imidazole. Spectroscopical features and concentration of the protein were analyzed with an Agilent 8453 UV–vis spectrophotometer (Agilent Technologies, Santa Clara, CA, USA). Protein concentration was calculated from the P450—CO complex spectrum upon reduction with sodium dithionite using an extinction coefficient of 91,000 M^{-1} cm^{-1}.[38]

2.4 | Cytochrome c assay

The nicotinamide cofactor preference of the reductase domain was investigated by following the reduction of the cytochrome c (50 μM final concentration). Experiments were carried out in triplicate at 25°C in potassium phosphate buffer (pH 6.8), with 9 nM enzyme and varying concentrations of cofactors (0–75 μM for NADPH and 0–2.0 mM for NADH). The reduction of cytochrome c was monitored with a SPECTROstar nano-microplate reader (BMG labtech, Aylesbury, UK) following the absorbance at 550 nm, using an extinction coefficient of 28,000 M^{-1} cm^{-1}. K_M and k_{cat} values were determined by fitting the data to the Michaelis–Menten equation by nonlinear regression rate using Sigma Plot.

2.5 | CYP116B5-fl structural models

The predicted 3D structure model of the full-length CYP116B5 was obtained from the AlphaFold DataBase (UniProt identifier: AF-G9BWN9-F1).[39,40] The amino acid sequence of CYP116B5-fl was aligned to the sequence of CYP116B46 using the pairwise sequence alignment tool (EMBL-EBI).[41] 3D models were created using the software PyMol.

2.6 | Catalytic activity assay

The catalytic activity of CYP116B5-fl, CYP116B5-hd, and the chimeric enzyme CYP116B5-SOX was studied using *p*-nitrophenol as substrate. Experiments were carried out using cell-free extracts, which were diluted to contain an enzyme concentration of 1 μM (CYP116B5-fl), 0.5 μM (CYP116B5-hd), and 0.25 μM (CYP116B5-SOX). The reaction mixture was prepared in 50 mM potassium phosphate (pH 6.8), containing respectively 2 mM NADPH, 2 mM H_2O_2 or 10 mM sarcosine, and a range of 0–1.6 mM of *p*-nitrophenol. Reactions were incubated for 30 min at 30°C and stopped by adding 1% trichloroacetic acid (TCA). Samples were then centrifuged for 5 min at 10,000 g, and the supernatant was transferred to an NUNC96 96-well microplates (Thermo Fisher, Waltham, MA, USA). Color development was achieved by adding 9 M NaOH. The production of *p*-nitrocatechol was quantified spectrophotometrically by measuring the absorbance at 515 nm with a SPECTROstar nano-microplate reader (BMG Labtech, Aylesbury, UK) using an extinction coefficient of 12,400 M^{-1} cm^{-1}.[42]

3 | RESULTS

3.1 | Expression, purification, and spectroscopical features of CYP116B5-fl

E. coli BL21 (DE3) cells harboring the expression vector pET-116B5FL were used to find the optimal condition of gene expression and protein production, which was analyzed by SDS-PAGE. Several expression conditions were explored by varying the concentration of IPTG (0–1 mM) and temperature (28 and 16°C). At 28°C the protein band could be found only in whole cell samples, but it was not visible in the soluble fractions (Figure 1A). CYP116B5-fl was successfully produced in a soluble form in the non-induced sample (0 mM IPTG) at low temperature (16°C) for 18 h (Figure 1B).

CYP116B5-fl was produced at 16°C for 18 h without adding IPTG. Figure 1C shows the SDS-PAGE analysis of the purified fractions after Ni-NTA affinity purification. The absorption spectrum of the purified oxidized enzyme shows the typical features of cytochromes P450

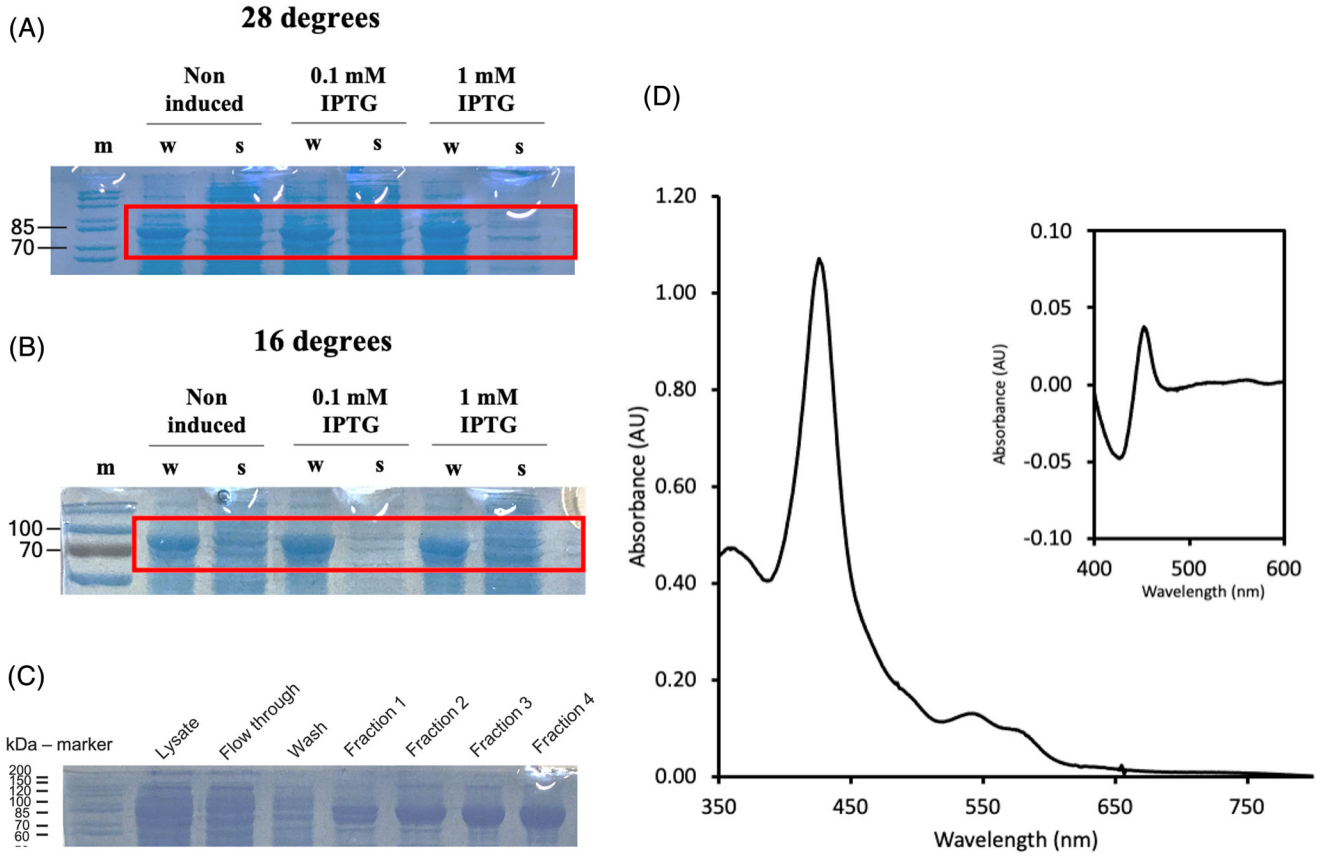

FIGURE 1 Expression, purification and spectroscopical features of CYP116B5-fl. SDS-PAGE analysis of protein expression trials at 16°C (A) and 28°C (B). Legend: m: molecular weight protein marker; w: whole cell sample; s: soluble proteins. Both gels include non-induced samples, and samples induced with 0.1 and 1 mM isopropyl β-D-thiogalactoside (IPTG). On the left side of the gels reference protein bands are indicated with the respective molecular weights expressed in kDa. Red rectangles indicate the area of the gel where the overexpressed protein is present at about 85 kDa. (C) SDS-PAGE analysis of protein purification showing the starting sample (lysate) and eluted fractions. (D) Spectroscopical features of pure CYP116B5-fl show the Soret peak at 424 nm, α and β peaks at 580 and 541 nm, flavin mononucleotide (FMN) at 450–475 nm. Inset: difference spectrum showing an increase at 450 nm generated by subtracting the spectrum of the oxidized CYP116B5-fl from the spectrum of the dithionite reduced form bubbled with CO.

(Figure 1D): Soret peak at 424 nm, α and β peaks at 580 and 541 nm. Moreover, the spectrum also shows a shoulder at 450–475 nm typical of oxidized flavin mononucleotide (FMN). The dithionite reduced form was bubbled with CO, causing a consequent shift of the Soret peak to 450 nm and the disappearance of the shoulder due to the reduction of the flavin.

3.2 | Nucleotide cofactor preference of CYP116B5-fl

The nicotinamide cofactor preference of the CYP116B5-fl reductase domain was investigated by following the reduction of the cytochrome c. The enzyme showed a preference toward NADPH over NADH. The calculated K_M were 8 ± 1 and 533 ± 14 μM, respectively, whereas k_{cat} values were 90.7 ± 3.8 and 152.9 ± 1.5 min^{-1}, respectively. The obtained Michaelis–Menten curves are shown in Figure 2.

3.3 | CYP116B5-fl structural analysis and CYP116B5-SOX chimera engineering

The 3D model of CYP116B5-fl predicted by AlphaFold DB was analyzed using Pymol and allowed to visualize the three-dimensional conformation of the three domains (Figure 3A). The primary structure of CYP116B5-fl was analyzed by aligning the amino acid sequence to the one of CYP116B46, which was used as a model for studying the electron transfer pathway from the reductase domain to the heme. The analysis revealed a 48% identity between the two enzymes. More specifically, the amino acid involved in the electron transfer were not found to be conserved (Figure 3B). The 3D models of Figure 3C,D indicate that the differences in the physicochemical properties of the amino acids may be responsible for the different activity of the two enzymes.

Starting from the native CYP116B5-fl (Figure 3E, i), the heme domain has been previously isolated obtaining a functional P450 that can serve as a peroxygenase (CYP116B5-hd) (Figure 3E, ii). In this work,

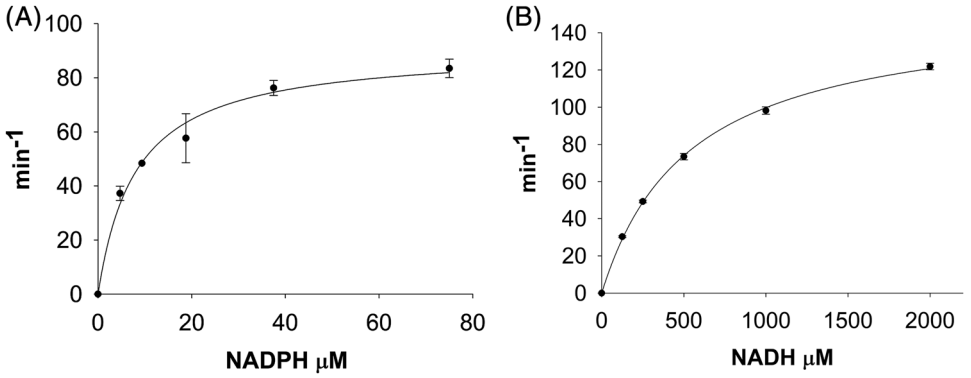

FIGURE 2 Kinetic parameters determination of CYP116B5-fl using NADPH (A) or NADH (B) as reductants and cytochrome c as electron acceptor. Error bars represent standard deviation; error bars are not visible when they are smaller than the data point symbols.

a new chimeric enzyme (CYP116B5-SOX) (Figure 3E, iii) was designed and obtained by switching the P450 reductase partner of CYP116B5-fl with the MSOX. The difference of three forms of CYP116B5 was investigated by measuring their catalytic activity.

3.4 | Catalytic activity toward *p*-nitrophenol of CYP116B5-SOX, CYP116B5-fl, and CYP116B5-hd

First, a preliminary test was performed to understand if CYP116B5-fl also undergoes peroxide shunt pathway using H_2O_2 as electron donor. The assay allowed to compare the relative activity of CYP116B5-fl in comparison to CYP116B5-hd in terms of *p*-nitrocatechol production. CYP116B5-fl showed a relative activity that was about 10% lower than the one of CYP116B5-hd. This confirmed that the P450 domain of CYP116B5-fl is able to use H_2O_2 in the same way as the isolated heme domain. The catalytic activity of the three enzymes CYP116B5-fl, CYP116B5-hd, and CYP116B5-SOX was then analyzed by measuring the production of *p*-nitrocatechol per mg of enzyme per minute, using a fixed concentration of 1.6 mM of *p*-nitrophenol as substrate. CYP116B5-SOX was the most active enzyme, followed by CYP116B5-hd and CYP116B5-fl, producing 93.54 ± 3.89, 28.97 ± 0.21, and 9.46 ± 0.19 μM *p*-nitrocatechol/mg enzyme/minute, respectively. If CYP116B5-SOX is used as a new benchmark for comparing the different enzyme systems, CYP116B5-hd and CYP116B5-fl can only reach 30% and 10% of the activity of the artificial construct (Figure 4). The kinetic parameters of the three forms of CYP116B5 toward *p*-nitrophenol were calculated and the Michaelis–Menten curves are reported in Figure 5. The resulting values of K_M were 121.35 ± 19.25 μM (CYP116B5-SOX), 108.15 ± 14.94 μM (CYP116B5-hd), and 218.65 ± 18.03 μM (CYP116B5-fl), while k_{cat}/K_M values were respectively 0.027, 0.008, and 0.001 μM^{-1} min^{-1}.

4 | DISCUSSION

In this work, we present a new strategy for the enhancement of the peroxygenase activity of CYP116B5 from *A. radioresistens*. Firstly, we characterized the full-length form of the enzyme (CYP116B5-fl) for the first time, and we carried out a detailed catalytic and structural comparison to other CYP116B isoenzymes. Secondly, we identified a new enzyme that was able to replace the native reductase domain and provide H_2O_2 to the heme domain instead of using NADPH. For this purpose, the MSOX from *Bacillus* sp. B0618[34–36] was fused to the C-terminus of the heme domain. MSOX catalyzes the oxidation of sarcosine to glycine and formaldehyde giving H_2O_2 as by-product. The activity of the new chimeric enzyme (CYP116B5-SOX) was compared to those of the isolated heme domain (CYP116B5-hd) and the newly characterized full-length form (CYP116B5-fl).

For CYP116B5-fl characterization, several tests were conducted aiming at finding the best condition for protein expression and recovery of the intact and active enzyme from the soluble fraction of the cell lysate. In contrast to CYP116B5-hd, which was produced at a temperature of over 20°C, CYP116B5-fl was only successfully produced in a soluble form only at low temperatures (16°C) (Figure 1A,B). Indeed, it is known that for the heterologous expression of some proteins, the gene induction at low temperature is particularly useful when the protein is readily degraded by proteases, aggregates, or is conveyed into inclusion bodies.[43] Moreover, a key point to produce a high amount of soluble CYP116B5-fl was the fine adjustment of gene expression. For this matter, different concentrations of IPTG (from 0 to 1 mM) were tested. The so-called leaky expression resulted to be crucial.[44] In fact, soluble protein could be obtained only in the condition where no IPTG was added to the medium and the promoter was not repressed, thus allowing a basal level of expression. Most P450s belonging to the subfamily CYP116B were expressed at temperatures higher than 20°C with a good production yield, particularly those from thermophilic microorganisms, which are stable and can perform their catalytic activity at high temperatures.[26] In our studies, only CYP116B5-hd could be produced at similar temperatures, indicating that the full-length form is more prone to unfolding or degradation in *E. coli*.

The spectroscopical features of the purified enzyme were found to be typical of the cytochromes from the same sub-family. When compared to CYP116B5-hd, the absorption spectrum of CYP116B5-fl shows an additional shoulder at 450–475 nm characteristic of the oxidized form of FMN (Figure 1D), thus confirming the incorporation

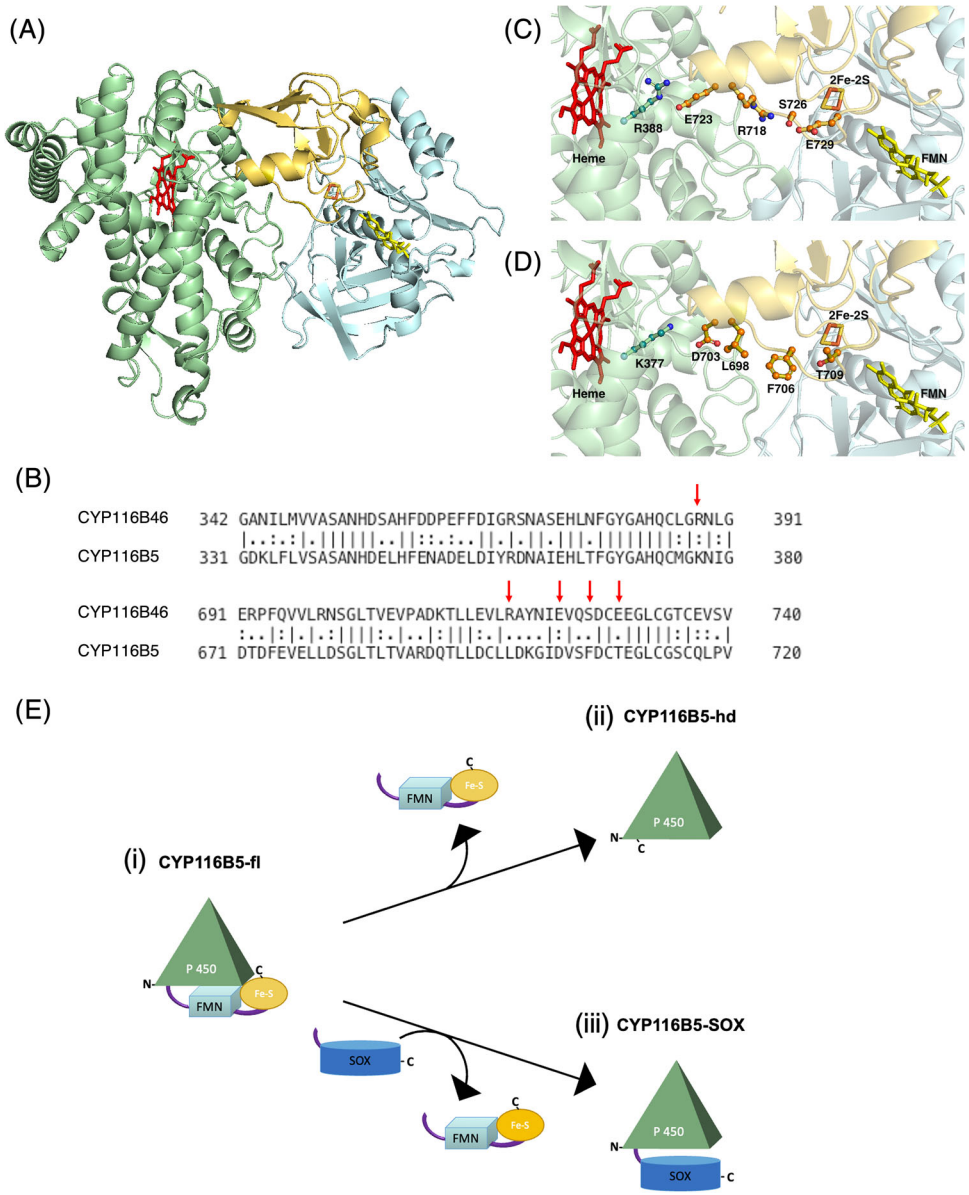

FIGURE 3 homology model of CYP116B5-fl and comparison with CYP116B46. The predicted structure of CYP116B5-fl (A) was obtained from AlphaFold DB. Color legend: heme domain (green) with heme (in red), reductase domain includes the flavin mononucleotide (FMN) domain (blue) with the FMN cofactor (in yellow), 2Fe-2S domain (pale yellow) with the 2Fe-2S cluster (in orange-yellow). (B) Sequence alignment between CYP116B46 and CYP116B5-fl with a highlight on the key residues involved on the electron transfer chain. The key residues of CYP116B46 (C) and the correspondent CYP116B5-fl residues (D) are labeled and are shown in ball and stick. (E) Forms of CYP116B5: (i) full-length form, (ii) isolated heme domain, and (iii) chimeric enzyme obtained by switching the reductase domain with monomeric sarcosine oxidase.

of the cofactor. The nicotinamide cofactor preference was determined spectroscopically by monitoring the reduction of cytochrome c as electron acceptor (Figure 2). The kinetic parameters of CYP116B5-fl and of all the previously characterized CYP116B isoenzymes[23,25–27,45,46] are reported in Table 1. For all CYP116 isoenzymes, the catalytic efficiencies (k_{cat}/K_M) were analyzed, as well as the cofactor preference ratio k_{cat}/K_M (NADPH/NADH). Similar to other CYP116B isoenzymes studied, also CYP116B5-fl showed a preference toward NADPH over NADH with a K_M value for NADPH of 8 μM, which falls in the range of the CYP116B isoenzymes (K_M = 0.9–9.3 μM). On the other hand, for CYP116B5 the k_{cat} value for NADPH was the lowest of the sub-family.

Recently, the first 3D structure of a full-length P450 of class VII (CYP116B46) was solved, providing insights into the interactions between the heme and reductase domains with a particular focus on the molecular mechanism of the electron transfer chain, which is crucial for the catalytic activity.[47] Four charged and one polar amino acid were identified as responsible for transferring the electrons from the iron-sulfur cluster to the heme. In order to evaluate possible differences between the two enzymes, an analysis was carried out by using a predicted structure of CYP116B5 obtained from AlphaFold DataBase (Figure 3A).[39,40] The amino acid sequence of the two enzymes was further analyzed using the pairwise sequence alignment tool (EMBL-

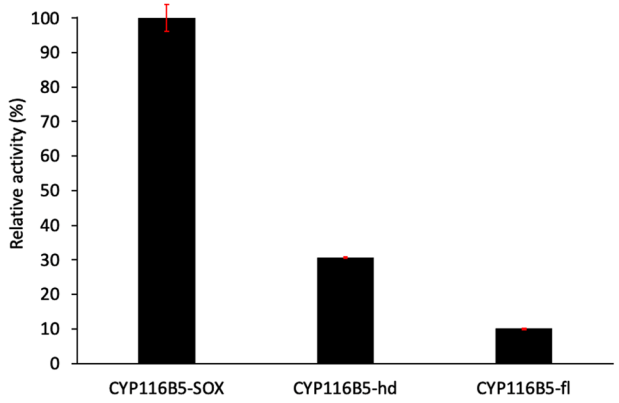

FIGURE 4 Relative activity of the enzymes CYP116B5-SOX, CYP116B5-hd and CYP116B5-fl expressed in percentage using CYP116B5-SOX as benchmark for comparison.

EBI).[41] The results show that the two enzymes share an identity of 48% but none of the five amino acids involved in the electron transfer chain is conserved (Figure 3B). The known electron transfer path from the 2Fe-2S cluster to the heme in CYP116B46 (Figure 3C) was analyzed and compared to the path of CYP116B5 (Figure 3D). The analysis shows that the first three amino acids in CYP116B64 (E729, S726, R718) are weakly similar to the ones of CYP116B5 (T709, F706, L698). On the other hand, the two amino acids that are located closer to the heme have the same type of charged side chain (E723, R388 in CYP116B46 and D703, K377 in CYP116B5), thus are considered to be strongly similar (Figure 3D). The evidence suggests that in CYP116B5 the electron transfer chain may be less efficient than the one of other CYP116B subfamily members but it cannot be excluded that a different molecular mechanism takes place and that for this cytochrome the electron transfer relies more on the structural arrangement of the domains, which is supposed to be more dynamic and may involve less or no amino acid residues.[8,48] The fact that the reductase domain of CYP116B5 has the lowest cofactor conversion rate among the CYP116B isoenzymes, added to the evidence that the electron transfer chain may be less efficient than the one of other CYP116B isoenzymes. This is also in support of the assumption that CYP116B5 may have a different evolutionary path and that it is more related to peroxygenases rather than monooxygenases. Indeed, the evolutionary analysis and the percentage of sequence identity of cytochromes CYP116 was previously studied and revealed that CYP116B5 is the least closely related to other members of the sub-family, having the lowest percentage of identity for both heme and reductase domains.[26,29] Further studies are certainly needed to elucidate the molecular differences of cytochromes belonging to this sub-family and to evaluate the ability of other CYP116B isoenzymes to perform their catalysis using the peroxide shunt.

The catalytic activity of CYP116B5-fl toward *p*-nitrophenol was subsequently investigated in comparison to CYP116B5-hd using cell-free extracts and NADPH or H_2O_2 as electron donor. The results show that this P450 is more efficient when it works as a peroxygenase (Figure 3). In fact, the catalysis driven by H_2O_2 in CYP116B5-hd is more than three-times higher than the one driven by NADPH in CYP116B5-fl. Similar studies have been carried out with P450 BM3, but with opposite results.[31] In the latter work, the NADPH-driven reaction of the full-length BM3 was higher than the H_2O_2-driven catalysis of its isolated heme domain (BMP). The wild-type P450 BM3 exhibits a low peroxygenase activity that can be improved by mutating specific residues starting from the phenylalanine in position 87, which plays a crucial role in accommodating H_2O_2 in the active site, and in stabilizing the enzyme in an H_2O_2 containing solution.[15–17] Previously, we analyzed and compared the sequence of CYP116B5 with other peroxygenases, including a mutant of P450 BM3 with improved peroxygenase activity, finding that these enzymes share identities or similarities in the position of amino acids that are crucial for the activity with hydrogen peroxide.[30]

As CYP116B5 is more efficient as a peroxygenase using H_2O_2, a new chimeric enzyme was designed in order to provide H_2O_2 to the heme domain with controlled and slow release over time via protein engineering. To this end, we have recently demonstrated that the use of MSOX in a chimeric system is beneficial for the catalytic activity as it provides H_2O_2 in a controlled manner and it prevents the rapid degradation of the heme.[37] Moreover, in the latter chimeric

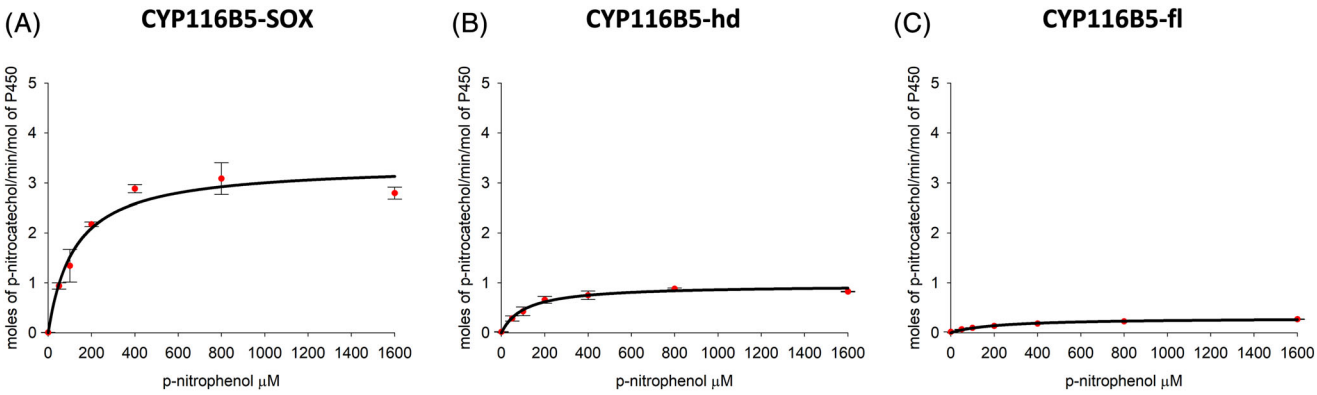

FIGURE 5 Kinetic parameters determination of CYP116B5-SOX using sarcosine (A), CYP116B5-hd using H_2O_2 (B), and CYP116B5-fl using NADPH (C) with *p*-nitrophenol as a substrate. Error bars represent standard deviation; error bars are not visible when they are smaller than the data point symbols.

TABLE 1 Kinetic properties of CYP116B using NADPH and NADH as reductants and cytochrome c as electron acceptor.

CYP116	Cofactor	K_M [M]	k_{cat} [min^{-1}]	k_{cat}/K_M [μM^{-1} min^{-1}]	Preference ratio k_{cat}/K_M (NADPH/NADH)
B1[45]	NADPH	0.9	151.1	167.8	1199
	NADH	399.1	57.1	0.14	
B2[46]	NADPH	6.6	2340	354.5	14
	NADH	40	960	24	
B3[23]	NADPH	3.4	764	224	78
	NADH	126	359	2.84	
B4[25]	NADPH	9.3	1236	132.9	4
	NADH	24.9	774	31	
B5[this work]	NADPH	8	90.7	11	39
	NADH	533	152.9	0.28	
B29[26]	NADPH	<1[a]	336	336	3.5
	NADH	2.7	258	95.5	
B46[26]	NADPH	2.5	2424	969.6	277
	NADH	482	1728	3.5	
B62[27]	NADPH	4.7	1320	280	200
	NADH	700	1020	1.4	
B63[26]	NADPH	5.4	4200	777	117
	NADH	640	4260	6.6	
B64[26]	NADPH	1.1	498	452	282
	NADH	213	342	1.6	
B65[26]	NADPH	8.4	4140	492	496
	NADH	1232	1224	0.99	

k_{cat} values that originally are reported in s^{-1}, here are converted in min^{-1}.
[a]This value was considered 1 for the calculation of k_{cat}/K_M.

system the catalytic activity of MSOX was comparable to the ones previously reported in the literature.[34] Indeed, several studies have shown how the catalytic activity of a P450 domain can be modulated by creating functional self-sufficient fusion proteins via the so-called "Molecular Lego" approach.[49–51] Moreover, biocatalytic systems that use peroxygenase can be supported by an in-situ production of H_2O_2 with beneficial effects.[52] In this work, the MSOX from *Bacillus* sp. B0618[34–36] was fused to the C-terminal of the heme domain to create the chimeric enzyme CYP116B5-SOX (Figure 3E). MSOX catalyzes the oxidation of sarcosine to glycine and formaldehyde giving H_2O_2 as by-products. The activity of CYP116B5-SOX was 10 times higher when compared to the activity of CYP116B5-fl and about three times higher than CYP116B5-hd (Figure 4), indicating that the modulation of H_2O_2 exposure to the catalytic domain is a key element for maintaining the activity at high level for longer time.

This work opens up the possibility of switching P450 partners in order to create different catalytic systems allowing for the selection of different molecules that serve as electron donors or precursors. Our results indicate that the applicability of this class of P450s for biocatalytic processes may be expanded, if they are used as peroxygenases. To-date, the peroxygenase activity of none of the other characterized CYP116B isoenzymes has been investigated or reported. Furthermore, these types of studies would certainly provide useful information that help understanding the differences on the molecular mechanisms of catalysis and on the evolutionary pathways of CYP116B enzymes.

AUTHOR CONTRIBUTIONS

Danilo Correddu: Conceptualization; investigation. Gianluca Catucci: Conceptualization; formal analysis; writing – review & editing. Daniele Giuriato: Investigation. Giovanna Di Nardo: Data curation. Alberto Ciaramella: Conceptualization; investigation. Gianfranco Gilardi: Conceptualization; funding acquisition; project administration; supervision; writing – review & editing.

ACKNOWLEDGMENTS

Open Access Funding provided by Universita degli Studi di Torino within the CRUI-CARE Agreement.

CONFLICT OF INTEREST STATEMENT

The authors declare no commercial or financial conflict of interest.

DATA AVAILABILITY STATEMENT

The data that support the findings of this study are available from the corresponding author upon reasonable request.

REFERENCES

1. Urlacher, V. B., & Girhard, M. (2019). Cytochrome P450 monooxygenases in biotechnology and synthetic biology biotechnology and synthetic biology. *Trends in Biotechnology*, *37*(8), 882–897. https://doi.org/10.1016/j.tibtech.2019.01.001
2. Di Nardo, G., & Gilardi, G. (2020). Natural compounds as pharmaceuticals: The key role of cytochromes P450 reactivity. *Trends in Biochemical Sciences*, *45*(6), 511–525. https://doi.org/10.1016/j.tibs.2020.03.004
3. Nelson, D. R. (2009). The cytochrome P450 homepage. *Human Genomics*, *4*(1), 59. https://doi.org/10.1186/1479-7364-4-1-59
4. Munro, A. W., Girvan, H. M., & McLean, K. J. (2007). Cytochrome P450–redox partner fusion enzymes. *Biochimica et Biophysica Acta (BBA) – General Subjects*, *1770*(3), 345–359. https://doi.org/10.1016/j.bbagen.2006.08.018
5. McLean, K. J., Luciakova, D., Belcher, J., Tee, K. L., & Munro, A. W. (2015). Biological diversity of cytochrome P450 redox partner systems. In E. G. Hrycay, & S. M. Bandiera (Eds.), *Monooxygenase, peroxidase and peroxygenase properties and mechanisms of cytochrome P450* (Vol. 851, pp. 299–317). Springer International Publishing. https://doi.org/10.1007/978-3-319-16009-2_11
6. Correddu, D., Di Nardo, G., & Gilardi, G. (2021). Self-sufficient class VII cytochromes P450: From full-length structure to synthetic biology applications. *Trends in Biotechnology*, *39*(11), 1184–1207. https://doi.org/10.1016/j.tibtech.2021.01.011
7. Ciaramella, A., Minerdi, D., & Gilardi, G. (2017). Catalytically self-sufficient cytochromes P450 for green production of fine chemicals. *Rendiconti Lincei*, *28*(1), 169–181. https://doi.org/10.1007/s12210-016-0581-z
8. Munro, A. W., Leys, D. G., McLean, K. J., Marshall, K. R., Ost, T. W. B., Daff, S., Miles, C. S., Chapman, S. K., Lysek, D. A., Moser, C. C., Page, C. C., & Dutton, P. L. (2002). P450 BM3: The very model of a modern flavocytochrome. *Trends in Biochemical Sciences*, *27*(5), 250–257. https://doi.org/10.1016/S0968-0004(02)02086-8
9. Di Nardo, G., & Gilardi, G. (2012). Optimization of the bacterial cytochrome P450 BM3 system for the production of human drug metabolites. *International Journal of Molecular Sciences*, *13*(12), 15901–15924. https://doi.org/10.3390/ijms131215901
10. Whitehouse, C. C. J., Bell, G. S., & Wong, L.-L. (2012). P450 BM3 (CYP102A1): Connecting the dots. *Chemical Society Reviews*, *41*(3), 1218–1260. https://doi.org/10.1039/C1CS15192D
11. Di Nardo, G., Fantuzzi, A., Sideri, A., Panicco, P., Sassone, C., Giunta, C., & Gilardi, G. (2007). Wild-type CYP102A1 as a biocatalyst: Turnover of drugs usually metabolised by human liver enzymes. *JBIC Journal of Biological Inorganic Chemistry*, *12*(3), 313–323. https://doi.org/10.1007/s00775-006-0188-4
12. Tsotsou, G. E., Sideri, A., Goyal, A., Di Nardo, G., & Gilardi, G. (2012). Identification of mutant Asp251Gly/Gln307His of cytochrome P450 BM3 for the generation of metabolites of diclofenac, ibuprofen and tolbutamide. *Chemistry – A European Journal*, *18*(12), 3582–3588. https://doi.org/10.1002/chem.201102470
13. Sideri, A., Goyal, A., Di Nardo, G., Tsotsou, G. E., & Gilardi, G. (2013). Hydroxylation of non-substituted polycyclic aromatic hydrocarbons by cytochrome P450 BM3 engineered by directed evolution. *Journal of Inorganic Biochemistry*, *120*, 1–7. https://doi.org/10.1016/j.jinorgbio.2012.11.007
14. Di Nardo, G., Dell'Angelo, V., Catucci, G., Sadeghi, S. J., & Gilardi, G. (2016). Subtle structural changes in the Asp251Gly/Gln307His P450 BM3 mutant responsible for new activity toward diclofenac, tolbutamide and ibuprofen. *Archives of Biochemistry and Biophysics*, *602*, 106–115. https://doi.org/10.1016/j.abb.2015.12.005
15. Cirino, P. C., & Arnold, F. H. (2003). A self-sufficient peroxide-driven hydroxylation biocatalyst. *Angewandte Chemie International Edition*, *42*(28), 3299–3301. https://doi.org/10.1002/anie.200351434
16. Cirino, P. C., & Arnold, F. H. (2002). Regioselectivity and activity of cytochrome P450 BM-3 and mutant F87A in reactions driven by hydrogen peroxide. *Advanced Synthesis & Catalysis*, *344*(9), 932–937. https://doi.org/10.1002/1615-4169(200210)344:9⟨932::AID-ADSC932⟩3.0.CO;2-M
17. Li, Q.-S., Ogawa, J., & Shimizu, S. (2001). Critical role of the residue size at position 87 in H2O2-dependent substrate hydroxylation activity and H2O2 inactivation of cytochrome P450BM-3. *Biochemical and Biophysical Research Communications*, *280*(5), 1258–1261. https://doi.org/10.1006/bbrc.2001.4261
18. Munro, A. W., McLean, K. J., Grant, J. L., & Makris, T. M. (2018). Structure and function of the cytochrome P450 peroxygenase enzymes. *Biochemical Society Transactions*, *46*(1), 183–196. https://doi.org/10.1042/BST20170218
19. Matsunaga, I., Yamada, M., Kusunose, E., Nishiuchi, Y., Yano, I., & Ichihara, K. (1996). Direct involvement of hydrogen peroxide in bacterial α-hydroxylation of fatty acid. *FEBS Letters*, *386*(2), 252–254. https://doi.org/10.1016/0014-5793(96)00451-6
20. Rude, M. A., Baron, T. S., Brubaker, S., Alibhai, M., Del Cardayre, S. B., & Schirmer, A. (2011). Terminal olefin (1-alkene) biosynthesis by a novel P450 fatty acid decarboxylase from Jeotgalicoccus species. *Applied and Environmental Microbiology*, *77*(5), 1718–1727. https://doi.org/10.1128/AEM.02580-10
21. Roberts, G. A., Grogan, G., Greter, A., Flitsch, S. L., & Turner, N. J. (2002). Identification of a new class of cytochrome P450 from a Rhodococcus sp. *Journal of Bacteriology*, *184*(14), 3898–3908. https://doi.org/10.1128/JB.184.14.3898-3908.2002
22. De Mot, R., & Parret, A. H. A. (2002). A novel class of self-sufficient cytochrome P450 monooxygenases in prokaryotes. *Trends in Microbiology*, *10*(11), 502–508. https://doi.org/10.1016/S0966-842X(02)02458-7
23. Liu, L., Schmid, R. D., & Urlacher, V. B. (2006). Cloning, expression, and characterization of a self-sufficient cytochrome P450 monooxygenase from Rhodococcus ruber DSM 44319. *Applied Microbiology and Biotechnology*, *72*(5), 876–882. https://doi.org/10.1007/s00253-006-0355-0
24. Li, A.-T., Zhang, J.-D., Xu, J.-H., Lu, W.-Y., & Lin, G.-Q. (2009). Isolation of Rhodococcus sp. strain ECU0066, a new sulfide monooxygenase-producing strain for asymmetric sulfoxidation. *Applied and Environmental Microbiology*, *75*(2), 551–556. https://doi.org/10.1128/AEM.01527-08
25. Yin, Y.-C., Yu, H.-L., Luan, Z.-J., Li, R.-J., Ouyang, P.-F., Liu, J., & Xu, J.-H. (2014). Unusually broad substrate profile of self-sufficient cytochrome P450 monooxygenase CYP116B4 from Labrenzia aggregata. *ChemBioChem*, *15*(16), 2443–2449. https://doi.org/10.1002/cbic.201402309
26. Tavanti, M., Porter, J. L., Sabatini, S., Turner, N. J., & Flitsch, S. L. (2018). Panel of new thermostable CYP116B self-sufficient cytochrome P450 monooxygenases that catalyze C—H activation with a diverse substrate scope. *ChemCatChem*, *10*(5), 1042–1051. https://doi.org/10.1002/cctc.201701510
27. Porter, J. L., Sabatini, S., Manning, J., Tavanti, M., Galman, J. L., Turner, N. J., & Flitsch, S. L. (2018). Cloning, expression and characterisation of P450-Hal1 (CYP116B62) from Halomonas sp. NCIMB 172: A self-sufficient P450 with high expression and diverse substrate scope. *Enzyme and Microbial Technology*, *113*, 1–8. https://doi.org/10.1016/j.enzmictec.2018.02.005
28. Donoso, R. A., Ruiz, D., Gárate-Castro, C., Villegas, P., González-Pastor, J. E., Lorenzo, V. D., González, B., & Pérez-Pantoja, D. (2021). Identification of a self-sufficient cytochrome P450 monooxygenase from Cupriavidus pinatubonensis JMP134 involved in 2-hydroxyphenylacetic

acid catabolism, via homogentisate pathway. *Microbial Biotechnology*, *14*(5), 1944–1960. https://doi.org/10.1111/1751-7915.13865
29. Minerdi, D., Sadeghi, S. J., Nardo, G. D., Rua, F., Castrignanò, S., Allegra, P., & Gilardi, G. (2015). CYP116B5: A new class VII catalytically self-sufficient cytochrome P450 from *Acinetobacter radioresistens* that enables growth on alkanes. *Molecular Microbiology*, *95*(3), 539–554. https://doi.org/10.1111/mmi.12883
30. Ciaramella, A., Catucci, G., Gilardi, G., & Di Nardo, G. (2019). Crystal structure of bacterial CYP116B5 heme domain: New insights on class VII P450s structural flexibility and peroxygenase activity. *International Journal of Biological Macromolecules*, *140*, 577–587. https://doi.org/10.1016/j.ijbiomac.2019.08.141
31. Ciaramella, A., Catucci, G., Di Nardo, G., Sadeghi, S. J., & Gilardi, G. (2020). Peroxide-driven catalysis of the heme domain of A. radioresistens cytochrome P450 116B5 for sustainable aromatic rings oxidation and drug metabolites production. *New Biotechnology*, *54*, 71–79. https://doi.org/10.1016/j.nbt.2019.08.005
32. Famulari, A., Correddu, D., Di Nardo, G., Gilardi, G., Chiesa, M., & García-Rubio, I. (2022). EPR characterization of the heme domain of a self-sufficient cytochrome P450 (CYP116B5). *Journal of Inorganic Biochemistry*, *231*, 111785. https://doi.org/10.1016/j.jinorgbio.2022.111785
33. Famulari, A., Correddu, D., Nardo, G. D., Gilardi, G., Chiesa, M., & García-Rubio, I. (2022). CYP116B5hd, a self-sufficient P450 cytochrome: A dataset of its electronic and geometrical properties. *Data in Brief*, *42*, 108195. https://doi.org/10.1016/j.dib.2022.108195
34. Wagner, M. A., & Jorns, M. S. (2000). Monomeric sarcosine oxidase: 2. Kinetic studies with sarcosine, alternate substrates, and a substrate analogue. *Biochemistry*, *39*(30), 8825–8829. https://doi.org/10.1021/bi000350y
35. Wagner, M. A., Khanna, P., & Jorns, M. S. (1999). Structure of the flavocoenzyme of two homologous amine oxidases: Monomeric sarcosine oxidase and N-methyltryptophan oxidase. *Biochemistry*, *38*(17), 5588–5595. https://doi.org/10.1021/bi982955o
36. Chlumsky, L. J., Zhang, L., & Jorns, M. S. (1995). Sequence analysis of sarcosine oxidase and nearby genes reveals homologies with key enzymes of folate one-carbon metabolism. *Journal of Biological Chemistry*, *270*(31), 18252–18259. https://doi.org/10.1074/jbc.270.31.18252
37. Giuriato, D., Correddu, D., Catucci, G., Di Nardo, G., Bolchi, C., Pallavicini, M., & Gilardi, G.. Design of a H2O2-generating P450SPα fusion protein for high yield fatty acid conversion. *Protein Science*, *31*(12), e4501.
38. Omura, T., & Sato, R. (1964). The carbon monoxide-binding pigment of liver microsomes: I. Evidence for its hemoprotein nature. *Journal of Biological Chemistry*, *239*(7), 2370–2378. https://doi.org/10.1016/S0021-9258(20)82244-3
39. Varadi, M., Anyango, S., Deshpande, M., Nair, S., Natassia, C., Yordanova, G., Yuan, D., Stroe, O., Wood, G., Laydon, A., Žídek, A., Green, T., Tunyasuvunakool, K., Petersen, S., Jumper, J., Clancy, E., Green, R., Vora, A., Lutfi, M., … Velankar, S. (2022). AlphaFold Protein Structure Database: Massively expanding the structural coverage of protein-sequence space with high-accuracy models. *Nucleic Acids Research*, *50*(D1), D439–D444. https://doi.org/10.1093/nar/gkab1061
40. Jumper, J., Evans, R., Pritzel, A., Green, T., Figurnov, M., Ronneberger, O., Tunyasuvunakool, K., Bates, R., Žídek, A., Potapenko, A., Bridgland, A., Meyer, C., Kohl, S. A. A., Ballard, A. J., Cowie, A., Romera-Paredes, B., Nikolov, S., Jain, R., Adler, J., … Hassabis, D. (2021). Highly accurate protein structure prediction with AlphaFold. *Nature*, *596*(7873), 7873. https://doi.org/10.1038/s41586-021-03819-2
41. Madeira, F., Pearce, M., Tivey, A. R. N., Basutkar, P., Lee, J., Edbali, O., Madhusoodanan, N., Kolesnikov, A., & Lopez, R. (2022). Search and sequence analysis tools services from EMBL-EBI in 2022. *Nucleic Acids Research*, *50*(W1), W276–W279. https://doi.org/10.1093/nar/gkac240
42. Fairhead, M., Giannini, S., Gillam, E. M. J., & Gilardi, G. (2005). Functional characterisation of an engineered multidomain human P450 2E1 by molecular Lego. *JBIC Journal of Biological Inorganic Chemistry*, *10*(8), 842–853. https://doi.org/10.1007/s00775-005-0033-1
43. Correddu, D., Montaño López, J. d. J, Vadakkedath, P. G., Lai, A., Pernes, J. I., Watson, P. R., & Leung, I. K. H. (2019). An improved method for the heterologous production of soluble human ribosomal proteins in *Escherichia coli*. *Scientific Reports*, *9*(1), Article1. https://doi.org/10.1038/s41598-019-45323-8
44. Mertens, N., Remaut, E., & Fiers, W. (1995). Tight transcriptional control mechanism ensures stable high-level expression from T7 promoter-based expression plasmids. *Biotechnology*, *13*(2), Article2. https://doi.org/10.1038/nbt0295-175
45. Warman, A. J., Robinson, J. W., Luciakova, D., Lawrence, A. D., Marshall, K. R., Warren, M. J., Cheesman, M. R., Rigby, S. E. J., Munro, A. W., & McLean, K. J. (2012). Characterization of Cupriavidus metallidurans CYP116B1 – A thiocarbamate herbicide oxygenating P450–phthalate dioxygenase reductase fusion protein. *The FEBS Journal*, *279*(9), 1675–1693. https://doi.org/10.1111/j.1742-4658.2012.08543.x@10.1002/(ISSN)1742-4658(CAT)VirtualIssues(VI)MolecularEnzymology2012
46. Roberts, G. A., Çelik, A., Hunter, D. J. B., Ost, T. W. B., White, J. H., Chapman, S. K., Turner, N. J., & Flitsch, S. L. (2003). A self-sufficient cytochrome P450 with a primary structural organization that includes a flavin domain and a [2Fe-2S] redox center. *Journal of Biological Chemistry*, *278*(49), 48914–48920. https://doi.org/10.1074/jbc.M309630200
47. Zhang, L., Xie, Z., Liu, Z., Zhou, S., Ma, L., Liu, W., Huang, J.-W., Ko, T.-P., Li, X., Hu, Y., Min, J., Yu, X., Guo, R.-T., & Chen, C.-C. (2020). Structural insight into the electron transfer pathway of a self-sufficient P450 monooxygenase. *Nature Communications*, *11*(1), Article1. https://doi.org/10.1038/s41467-020-16500-5
48. Jeffreys, L. N., Pacholarz, K. J., Johannissen, L. O., Girvan, H. M., Barran, P. E., Voice, M. W., & Munro, A. W. (2020). Characterization of the structure and interactions of P450 BM3 using hybrid mass spectrometry approaches. *Journal of Biological Chemistry*, *295*(22), 7595–7607. https://doi.org/10.1074/jbc.RA119.011630
49. Catucci, G., Ciaramella, A., Di Nardo, G., Zhang, C., Castrignanò, S., & Gilardi, G. (2022). Molecular Lego of human cytochrome P450: The key role of heme domain flexibility for the activity of the chimeric proteins. *International Journal of Molecular Sciences*, *23*(7), Article7. https://doi.org/10.3390/ijms23073618
50. Sadeghi, S. J., Meharenna, Y. T., Fantuzzi, A., Valetti, F., & Gilardi, G. (2000). Engineering artificial redox chains by molecular 'Lego'. *Faraday Discussions*, *116*(0), 135–153. https://doi.org/10.1039/B003180L
51. Gilardi, G., Meharenna, Y. T., Tsotsou, G. E., Sadeghi, S. J., Fairhead, M., & Giannini, S. (2002). Molecular Lego: Design of molecular assemblies of P450 enzymes for nanobiotechnology. *Biosensors and Bioelectronics*, *17*(1), 133–145. https://doi.org/10.1016/S0956-5663(01)00286-X
52. Paul, C. E., Churakova, E., Maurits, E., Girhard, M., Hollmann, F., & Urlacher, V. B. (2014). In situ formation of H2O2 for P450 peroxygenases. *Bioorganic & Medicinal Chemistry*, *22*(20), 5692–5696. https://doi.org/10.1016/j.bmc.2014.05.074

How to cite this article: Correddu, D., Catucci, G., Giuriato, D., Di Nardo, G., Ciaramella, A., & Gilardi, G. (2023). Catalytically self-sufficient CYP116B5: Domain switch for improved peroxygenase activity. *Biotechnology Journal*, e2200622. https://doi.org/10.1002/biot.202200622